Modeling impurity-assisted chain creation in noble-metal break junctions

2012 J. Phys.: Condens. Matter 24 135501

(http://iopscience.iop.org/0953-8984/24/13/135501)

IOP Publishing Journal of Physics: Condensed Matter
J. Phys.: Condens. Matter **24** (2012) 135501 (11pp) doi:10.1088/0953-8984/24/13/135501

Modeling impurity-assisted chain creation in noble-metal break junctions

S Di Napoli[1,2], A Thiess[3], S Blügel[3] and Y Mokrousov[3]

[1] Departamento de Física de la Materia Condensada, CAC-CNEA, Avenida General Paz 1499, (1650) San Martín, Pcia. de Buenos Aires, Argentina
[2] Consejo Nacional de Investigaciones Científicas y Técnicas, CONICET, Buenos Aires, Argentina
[3] Peter Grünberg Institut and Institute for Advanced Simulation, Forschungszentrum Jülich and JARA, D-52425 Jülich, Germany

E-mail: dinapoli@tandar.cnea.gov.ar

Received 23 November 2011, in final form 13 January 2012
Published 6 March 2012
Online at stacks.iop.org/JPhysCM/24/135501

Abstract
In this work we present the generalization of the model for chain formation in break junctions, introduced by Thiess *et al* (2008 *Nano Lett.* **8** 2144), to zigzag transition-metal chains with s and p impurities. We apply this extended model to study the producibility trends for noble-metal chains with impurities, often present in break junction experiments, namely, Cu, Ag and Au chains with H, C, O and N adatoms. Providing the material-specific parameters for our model from systematic full-potential linearized augmented plane-wave first-principles calculations, we find that the presence of such impurities crucially affects the binding properties of the noble-metal chains. We reveal that both the impurity-induced bond strengthening and the formation of zigzag bonds can lead to a significantly enhanced probability for chain formation in break junctions.

(Some figures may appear in colour only in the online journal)

1. Introduction

Quantum transport in nanoscale and atomic-scale objects has recently become one of the most researched areas in modern physics, owing to the vast possible applications in technology. On the most exciting side, electronic properties of one-dimensional (1D) systems such as atomic chains and molecular wires often lead to fascinating transport properties, which were predicted to occur theoretically and could be observed experimentally. After years of research, the material versatility of the class of 1D systems still remains rather poor, however. This can be mainly attributed to the fact that it proved to be rather difficult to produce and sustain a free-standing, or even deposited, chain experimentally. One of the most promising experimental techniques developed over the last decade, which allows one to produce 1D structures and measure their transport properties, lies in investigating the mechanically controllable break junctions (MCBJ) [2].

In a typical break junction experiment, two pieces of material which are initially in contact are pulled apart while the conductance of the system is measured. During the process of pulling, several atoms may be extracted from the leads, forming a free-standing finite 1D chain [2]. With this technique it has been possible to create monatomic chains with a length of 5–10 atoms in Ir [3], Pt [2], and Au [4–6] break junctions. The ability to create similarly long chains in break junctions of other metals has been greatly hindered so far. For example, it has been demonstrated that the tendency for chain creation in lighter 3d and 4d transition metals (TMs) is significantly lower than in 5d TMs. This trend was later explained based on the relativistic enhancement of mass in heavier elements with a corresponding analogy to the reconstruction of the low-index surfaces of the 5d TMs.

In recent years it has become evident that it is possible to strengthen the bonds in a suspended chain and achieve a higher degree of chain producibility by adding external absorbates during the process of chain formation. This opens a new possibility for achieving the desired versatility of one-dimensional systems with different properties produced in MCBJ experiments. In a key experiment [7], Thijssen *et al* observed such an enhanced tendency towards chain elongation for Au, Ag and Cu break junctions with oxygen present in

the atmosphere. Moreover, the effect of other impurities, such as H, B, C, N and S, on the creation of Au chains has been considered, while stable and strong bonding between the Au and impurity atoms has been demonstrated [8–10]. Physically, such a situation can be explained based on a well-known observation that low-coordinated noble-metal (NM) atoms are chemically more reactive than in the bulk and thus their chains are expected to be even more reactive than nanoparticles [11, 12].

Experimental advances in producing longer chains with the aid of impurities of various physical and chemical natures call for an appropriate theoretical description. Taking into account the complexity of MCBJ experiments, the aim of a proper chain formation theory lies mainly in guiding future successful experiments and extending the material base for further studies. In this respect the predictive power of density functional theory (DFT) first-principles, or *ab initio*, techniques is particularly valuable. Treating the complicated process of a chain's stretching, elongation and eventual breaking upon pulling the electrodes apart in an atmosphere contaminated with various elements is an extremely challenging task even for the fastest first-principles methods. The main obstacle here is the necessity to describe simultaneous restructuring of hundreds of atoms in real time. Due to computational limitations, *ab initio* studies of impurity-assisted chain formation have so far focused mainly on the stability, mechanical and electronic properties of clean and contaminated infinite chains of transition metals [13–16]. This situation calls for the development of an effective model which is able to utilize the results of first-principles calculations of simplified systems for the purpose of describing the chain formation on a level which allows extension of the material base for future MCBJ experiments with a reasonable computational effort.

Recently, Thiess *et al* introduced a model ('chain formation model' in the following) able to provide the probability of chain's elongation in a break junction using only a limited number of parameters which can be extracted from first-principles calculations of a perfect infinite chain and idealized leads. Using this model, the authors of [1] analyzed the chemical trend of chain creation in break junctions of 3d, 4d and 5d transition metals, arriving at a qualitative agreement with experiments and unraveling the physics behind the observed trends [1]. An attractive feature of this approach lies in the ability to visualize the process of chain formation by referring to phase diagrams for the probability of elongation as a function of a chain's stretching and the number of atoms in the chain. Additionally, the obtained chemical trends can be understood based on a small number of element-specific parameters. Using this model, the tendency for chain elongation in linear Au–O chains has been predicted to be stronger than in pure Au chains, in accordance with experiments [1].

In this work, we systematically apply the chain formation model for a detailed study of the trends in the formation of Cu, Ag and Au chains in pure break junctions as well as Cu, Ag and Au break junctions with the atmosphere contaminated by H, C, N, and O impurities. Additionally, we extend the chain formation model to the case of a geometrically more complex zigzag arrangement of the atoms in the chain. In particular, we find that some of the chains exhibit a finite probability for elongation under significant tension in the linear regime as well as for the zigzag arrangement. While the probability of the chain's elongation in the zigzag regime is rather small, it has an advantage that it is more robust with respect to breaking. Overall, we predict that incorporation of all considered impurities, even hydrogen, into the noble-metal (NM) chains results in an increased probability for chain elongation when compared to the pure chains of NM elements. We also observe that although NM chains with s-type H impurities display wide regions of finite probability for elongation as a function of strain, this probability is much smaller than that for NM chains with p-type impurities. Remarkably, our calculations predict a noticeably higher tendency towards chain elongation in Cu and Au contaminated chains than in Ag chains.

The paper is organized as follows. In section 2 we provide the details of our DFT first-principles calculations. In section 3 we analyze the energetics and structural properties of linear, zigzag and dimerized single-atom NM chains and NM chains with H, C, N and O impurities. After this, in section 4 we present the definition and the details of the model we use to estimate the tendency for chain elongation, as well as its generalization to the case of the zigzag geometry. Finally, in section 5 we analyze the process of chain formation in break junctions of NMs, pure and with impurities, and compare the predicted trends. A summary and conclusions are given in section 6.

2. Computational details

For our density functional theory first-principles calculations we employed the full-potential linearized augmented plane-wave (FLAPW) method for 1D systems [17], as implemented in the FLEUR code [18] within the (rev-PBE) generalized gradient approximation (GGA) to the exchange–correlation potential. The choice of the GGA is motivated by the fact that it is better suited to the description of exchange and correlation in low-dimensional geometries than the local density approximation (LDA), while our calculations show that the chain properties are moderately affected by the choice of the functional and the chain formation trends are rather robust with respect to the choice of the exchange–correlation parametrization. The FLAPW basis functions were expanded up to $k_{\max}$ of 4.0 bohr^{-1} and we used 32 k points in one half of the 1D Brillouin zone for our self-consistent calculations. The diameter of the cylindrical boundary between the interstitial and vacuum regions, D_{vac}, and the auxiliary in-plane lattice constant, $\tilde{D}$, were set to 8.3 bohr and 9.9 bohr, respectively (for details of the method and spatial partitioning within the 1D FLAPW scheme see [17]). The muffin-tin radii were set to 1.90 bohr for Au (with local orbitals for the 5s and 5p states), 2.0 bohr for Ag and Cu, and 1.0 bohr for the impurities. These values were chosen to guarantee the required accuracy as well as to enable a comparison between the total energies of the zigzag chains with a wide range of the angle α, see

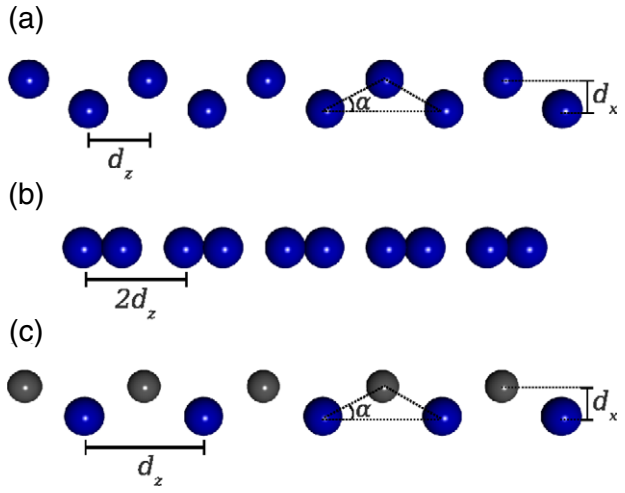

Figure 1. Schematic structure of (a) single-atom planar zigzag chains, (b) single-atom dimerized chains and (c) planar zigzag chains with impurities. The noble atoms are represented by large blue spheres, while smaller gray spheres stand for the impurity atoms.

figure 1. For our calculations we neglected the effect of the spin–orbit interaction, since its effect on the energetics of the chain formation was shown to be negligible [19, 20].

We set the coordinate system such that the chain axis is aligned along the z axis, and considered a two-atom unit cell to allow for zigzag and dimer arrangements, which are depicted schematically in figure 1. In the case of dimerized chains the distance d_z is the distance between the two neighboring unit cells, while the atoms are positioned strictly along the z-axis. In the case of zigzag chains, which are the primary focus of our study, the distance d_z is the distance between atoms of the same type along the z-axis, while the distance d_x is the distance between the two rows of atoms along the x-axis, with the chain lying in the xz-plane. The zigzag angle α is thus given by $\tan\alpha = d_x/d_z$ for pure NM chains and $\tan\alpha = 2d_x/d_z$ for NM chains with impurities. Note that in our calculations we assumed that in the zigzag configuration each atom is equidistant from its first nearest neighbors. In an experiment, the scope of the chain structures formed is, of course, much wider than the arrangements we consider in the current work. On the other hand, the choice of highly symmetric linear and zigzag chains that we consider is motivated by the following two considerations: (i) it allows us to perform an extensive amount of *ab initio* calculations keeping the computational load reasonable, and (ii) it allows for a transparent analysis of the structural properties of the chains in break junctions and a simpler understanding of the derived trends of chain formation.

3. Energetics

One of the purposes of our work is to understand the role of the geometric structure in chain formation taking into account energetics considerations. From this starting point we analyze the particular role of environmental impurities in the chain formation process. In order to achieve this goal, first, we performed systematic total energy calculations as a function of both the interatomic parameters, d_z and d_x (cf figure 1). For each d_z we performed a total energy calculation for at least five different d_x values. On the basis of these calculations we interpolated the two-dimensional energy profile in the d_z–d_x plane, from which we extracted the effective minimum energy curves as a function of d_z, $\varepsilon(d_z) = \min_{d_x} \varepsilon(d_z, d_x)$.

Our results for the noble-metal Cu, Ag and Au single-atom chains are summarized in figure 2, where the total energy and the zigzag α-angles are plotted as a function of d_z. The corresponding energies of the single-atom infinite linear and dimerized chains are also presented for comparison. As can be seen from this figure, in all three cases the zigzag structures with large values of the α-angle are more stable than the linear configurations, in agreement with previous studies [21–23]. All energy profiles display a characteristic two-well structure, where the first minimum corresponds to α-angles in the vicinity of 60°. In this configuration, each atom interacts strongly not only with its 'chain' first nearest neighbors along the z-axis, but also with the second nearest neighbors. The second minimum in the total energy curves, which is clearly pronounced in particular for Au and Cu, occurs for the values of α at around 25°, corresponding to a zigzag structure with each atom interacting mainly with its two first nearest neighbors. While the zigzag angle falls off rapidly to zero for d_z above 5.0 bohr for all chains, this decay is more abrupt for the case of Ag chains. As far as the dimerization is concerned, we find that the chains tend to dimerize when elongated above a d_z of ≈5.5 bohr, with a modest gain in energy as compared to the linear configuration for $5.5 < d_z < 6.5$ bohr. As we shall see in the following, when the interatomic distance lies in this interval, the chains are already very prone to breaking; thus, we do not consider the effect of dimerization on the chain formation considered in the following sections.

Next, we follow the same procedure for the case with an impurity in the two-atom unit cell, as shown schematically in figure 1(c). In figure 3 we present the evolution of the minimal total energy and corresponding zigzag angle with d_z in Cu, Ag and Au chains with H, C, N, and O impurities (NM–X chains). Note that the energy profiles are shifted in this figure with respect to each other along the y axis for better visibility. From figure 3 we observe that the behavior of the total energy is different as a function of d_z for s (H) and p impurities (C, N, O). In the latter case the global minimum in energy occurs for the linear configuration ($\alpha = 0°$) and the second local energy minimum can be seen also for the zigzag planar geometry with comparatively large angles α in the range of 30°–40°. This is in contrast to the pure NM chains, for which two energy minima are also present, yet they both correspond to zigzag geometry with profound energetic preference for higher α-angles, see figure 2. On the other hand, for NM–H chains the zigzag structure exhibits the global and only energy minimum, although the values of the zigzag angle are rather small, namely, $\alpha \approx 12°$ (Au–H), $\alpha \approx 6°$ (Ag–H) and $\alpha \approx 10°$ (Cu–H). We can therefore conclude that the presence of impurities in NM break junctions leads to an effective straightening of the bonds in the chain with energetically

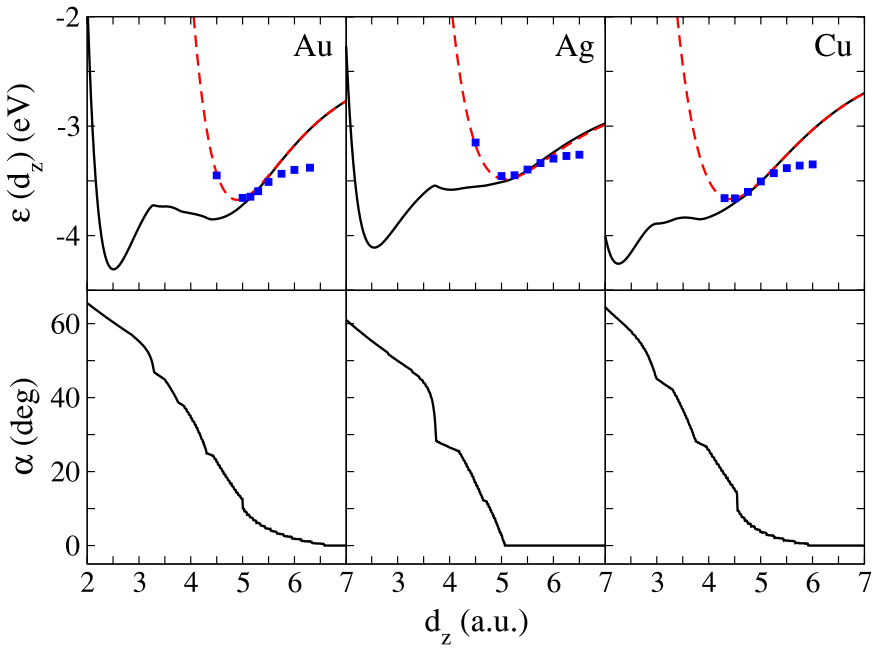

Figure 2. Upper panel: the minimal total energy ε (per atom) as a function of d_z for Au (left), Ag (middle) and Cu (right). The dashed red lines correspond to the total energies of the linear infinite single-atom chains, the solid black lines mark the total energies of the chains in the zigzag configuration, while the filled squares stand for the total energy profiles of the dimerized chains. Lower panel: the evolution of the corresponding zigzag α-angles.

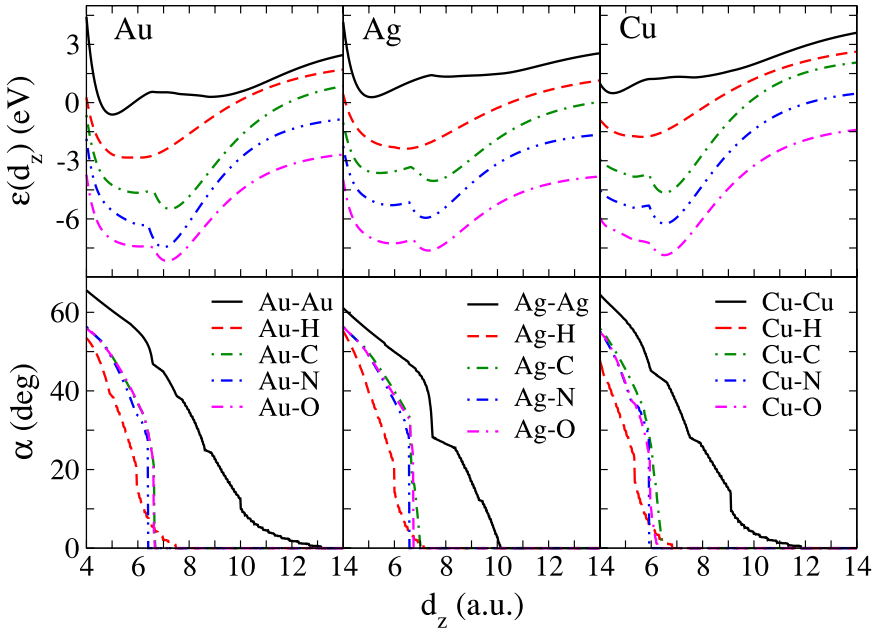

Figure 3. Upper panel: the minimal total energy (per unit cell) as a function of d_z for Au (left), Ag (middle) and Cu (right). For better comparison, the energy curves are rigidly shifted with respect to each other. Lower panel: the evolution of the corresponding zigzag α-angles.

favored configurations which are linear or exhibit small zigzag angles.

A common feature for all Ag–X chains, which can be seen in figure 3, is the smaller slope of the energy curves as a function of d_z, when compared to the corresponding Cu–X and Au–X cases. Such 'softening' of the $\varepsilon(d_z)$ profile can be seen already for pure Ag chains, when compared to Au and Cu chains, especially in the vicinity of the global zigzag minimum, figure 2. The reason behind this phenomenon lies in the fact that the d states of Ag are situated much lower in energy than the s states, which solely determine the character of the electronic states in the vicinity of the Fermi energy (E_F). In the case of Au and Cu, the d states are positioned higher in energy and overlap with the s states at the E_F, providing

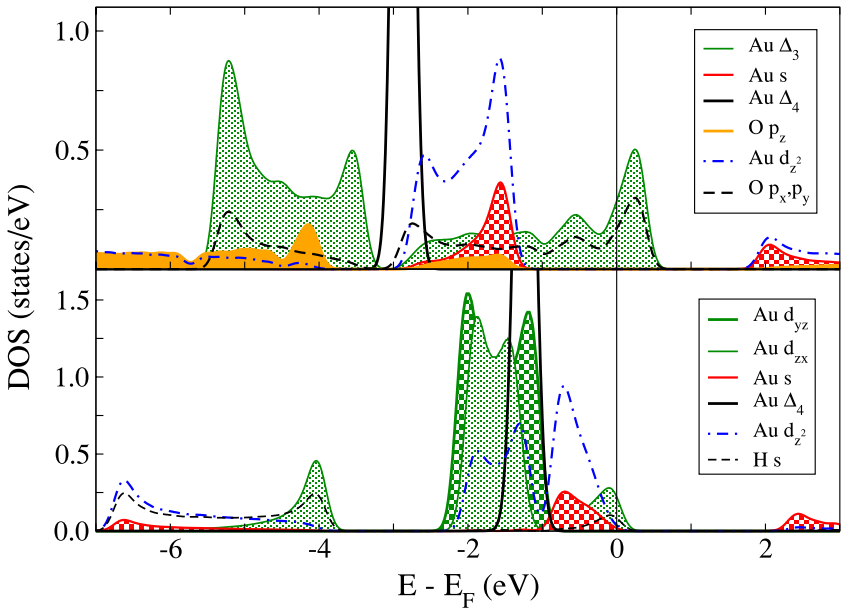

Figure 4. Atomically resolved densities of states for a Au–O chain with $d_z = 7.25$ bohr and $\alpha = 0°$ (top), and a Au–H chain with $d_z = 6.0$ bohr and $\alpha \approx 18°$ (bottom). The densities of states are additionally decomposed into the contributions coming from s, p and d states of different symmetries.

an additional channel for hybridization and bonding between the atoms. Correspondingly, the bonding in the chains of Ag atoms is somewhat weaker than in those made of Au and Cu. Such weakening of bonding and softening of the energy profile for Ag in comparison to Au and Cu was also observed for linear infinite chains and in bulk, cf [24] and citations therein.

In order to understand the difference in the structural properties of NM chains with s and p impurities, we consider the density of states (DOS) of Au–O ($d_z = 7.25$ bohr, $\alpha = 0°$) and Au–H ($d_z = 6.0$ bohr, $\alpha \approx 18°$) chains in close to equilibrium configurations, presented in figure 4. In this plot, the DOS is additionally decomposed into atomic (Au or X) and orbital s, p and d contributions. By looking at the DOS of the Au–O chain first, we observe that for the linear arrangement of the atoms in the chain the bonding of the atoms of Au and O is the strongest owing to the pronounced directionality of the oxygen's valence p orbitals. In this case the overlap between the s and d_{z^2} orbitals of Au and p_z orbital of O along the chain axis, as well as p_x and p_y oxygen orbitals with Au d states of Δ_3 symmetry (d_{zx} and d_{yz} orbitals) is the largest, which can be seen from the DOS (upper panel in figure 4). This leads to a pronounced minimum in the total energy for the linear regime. On the other hand, the hydrogen s orbital lacks the directionality of the p orbitals of oxygen atoms. In the linear case, brought into contact with Au atoms, the H s state can hybridize only with the corresponding Au states of the same Δ_1 symmetry, namely 6s and $5d_z$ states, while the states of the Δ_3 and Δ_4 (d_{xy} and $d_{x^2-y^2}$) symmetry would remain non-bonding. Upon transition to a zigzag configuration, the cylindrical symmetry of the chain is broken and the hybridization between the hydrogen s and Au Δ_3 orbitals occurs since it is not any longer forbidden by symmetry, as can be seen from the DOS in the lower panel of figure 4. This additional channel for bonding in the chain energetically favors the zigzag arrangement of H and Au atoms, although the magnitude of the zigzag angle is limited by the small radius of the 1s hydrogen orbital. Noticeably, in both cases the Δ_4 Au orbitals, which lie in the plane perpendicular to the chain axis, remain non-bonding, figure 4. The difference in the DOS of Ag and Cu chains with s and p impurities is similar to the case of Au, exhibiting the overall features discussed above and shown in figure 4.

4. Model of chain formation

During the process of stretching and chain formation in an MCBJ experiment, the atoms are extracted from the leads upon pulling them apart, and form a chain consisting of several atoms. Owing to the complex relaxations of hundreds of atoms during this process, its rigorous description from first-principles is an extremely challenging task. Moreover, the exact structure of the electrodes is normally unknown, which introduces a great deal of uncertainty in the initial configuration of the system. In the past, several approaches to overcome these obstacles were taken, among which the most successful ones lie in employing the molecular dynamics technique to tackle the chain formation process [13, 25–28]. In this work we choose a different path, and extend a simple model of chain formation proposed by Thiess *et al* [1], which is based on general total energy arguments. The applicability of this model to description of the complicated MCBJ chain formation process has been demonstrated for transition metals [1, 19].

According to the chain formation model, we divide the system into two regions: the leads and the suspended chain. The electronic structures of the two parts are considered separately from an *ab initio* approach, thus neglecting their

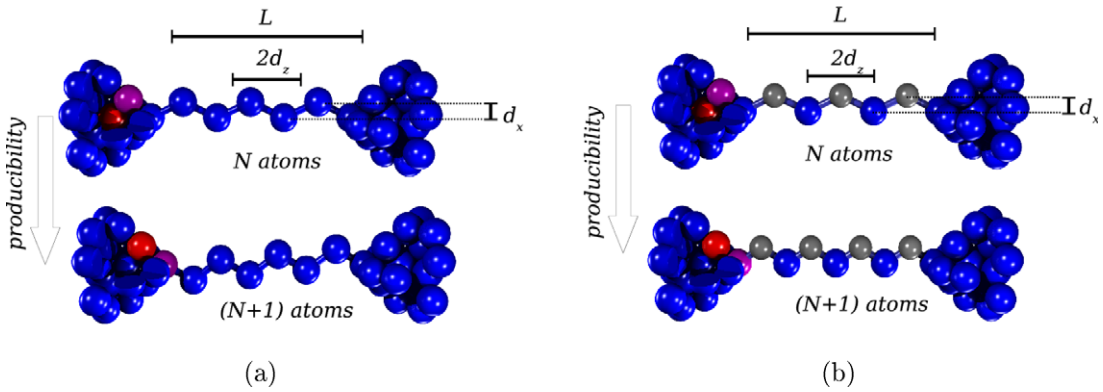

Figure 5. Sketch of the producibility (P) criterion in suspended single-atom chains (a) and in suspended chains with impurities (b).

mutual influence. This approximation becomes increasingly better when going to the limit of longer chains, which are the focus of our study. The process of chain formation is monitored by following the change in the total energy of an atom that is transferred from the lead into the chain upon chain elongation. To estimate this total energy change we assume that upon the transfer of the atom from the lead into the chain the only parameter which is changed in the system is the interatomic distance d between the atoms in the chain, while the length of the chain L and the structure of the leads remain the same. This is the so-called rapid reformation approximation (RRA) [6, 29, 30, 1]. Moreover, we suppose that the transfer of a lead atom into the wire happens instantaneously at a certain time t_i, when the energy of the transferred atom and its coordinates change suddenly from their values inside the lead to the corresponding values inside the chain. We also assume that between two consequent elongation events at times t_i and t_{i+1} the pulling of the electrodes apart results only in a smooth change of the chain's interatomic distance d.

In figure 5 we show a sketch of the system under consideration, where the two figures for each of the situations correspond to the initial and final states of the process of chain elongation. To analyze the producibility of the chain we compare the total energies of the initial and final configurations in the process of pulling one lead atom into the chain, where L is the distance between the leads. A successful chain elongation will be translated into the following total energy relation, the criterion for producibility (P-criterion):

$$(N+1)\epsilon(d) \geq \Delta E_{\text{lead}} + (N+2)\epsilon(\tilde{d}) \qquad (1)$$

where $d = L/(N+1)$ and $\tilde{d} = L/(N+2)$ are the chain interatomic distances before and after the elongation, respectively, and $N+1$ is the number of bonds in a chain of N atoms. The binding energy of the suspended chain, $\epsilon(d)$, is defined from the binding energy of the infinite wire with interatomic distance d, $E_{\text{W}}(d) = E_{\text{W}}(d_0) + \epsilon(d)$ (we always have two atoms in the unit cell), relative to the wire's cohesive energy at equilibrium interatomic distance d_0, $E_{\text{W}}(d_0)$, which implies $\epsilon(d) > 0$.

The chain formation energy in equation (1) is given by $\Delta E_{\text{lead}} = E_{\text{W}}(d_0) - E_{\text{lead}}$, where E_{lead} denotes the cohesive energy of an atom inside the lead. To calculate E_{lead} we perform a bulk calculation of the total energy for each chemical element at its corresponding equilibrium lattice constant, E_{bulk}, and a bulk calculation of the total energy of the isolated atom, E_∞, to get $\Delta E_{\text{bulk}} = E_\infty - E_{\text{bulk}}$. Taking into account the surface energies calculated by Skriver and Rosengaard [31], $\Delta E_{\text{surf}} = E_{\text{surf}} - E_{\text{bulk}}$, we defined $E_{\text{lead}} = \Delta E_{\text{bulk}} - \Delta E_{\text{surf}} = E_\infty - E_{\text{surf}}$, where E_{surf} is calculated analogously to E_{bulk} for an atom at the surface of a certain crystallographic orientation. At finite temperatures, ΔE_{lead} corresponds to the difference between the chemical potentials of the lead and of the infinite wire. Typically, $\Delta E_{\text{lead}} > 0$. If the P-criterion (equation (1)) is satisfied the system tends to increase the number of atoms in the chain by one. One can rewrite the P-criterion in the following way:

$$E^*(d, N) = (N+1)\epsilon(d) - \Delta E_{\text{lead}} + (N+2)\epsilon(\tilde{d}) \qquad (2)$$

where $E^*(d, N)$ is a function of the interatomic distance and the number of atoms in the chain. If $E^*(d, N) > 0$ the P-criterion is satisfied and the chain can increase by one atom for that particular pair of parameters (d, N).

To apply the P-criterion to suspended chains it is useful to fit the chain binding energy $\epsilon(d)$ with an analytical function. As the phase space of possible structural arrangements of the wires is two-dimensional, we calculated the binding energy for several d_x and d_z distances in the wire (see figure 1), and fitted each energy curve with the analytical Morse potential [1], interpolating the minimum energy curve from these data for all considered wires, as explained in section 3. Thus, the binding energies participating in equations (1) and (2) are the energy curves shown in figures 2 and 3.

We define the string tension, or force $F(d)$, as the slope of the binding energy with respect to the distance between the atoms along the z-axis $d = d_z$ (see figure 5):

$$F(d) = F(d_z) = \frac{\delta\epsilon(d_z)}{\delta d_z}. \qquad (3)$$

From equations (1) and (3) we can deduce that there are two main parameters which compete and which determine whether a chain can be increased by one atom [1]. These are (i) the energy cost of bringing an atom from the lead into the chain, ΔE_{lead}, and (ii) the break force F_0, which is

the maximum of the string tension occurring at the so-called inflection point $\hat{d}$, that is, $F_0 = F(\hat{d})$. The inflection point gives an estimate of how far an ideal infinite chain can be stretched until it breaks from the maximum break force due to long-wavelength perturbations [1]. Physically, a successful chain elongation event will occur when the following happens. As the chain is stretched, the energy of the system increases up to the point where a lead atom overcomes the chain formation barrier, ΔE_{lead}, and enters the chain. This relaxes the distance in the chain from d to $\tilde{d}$ and lowers the total energy of an atom in the wire, $E_{\text{W}}(\tilde{d}) < E_{\text{W}}(d)$. The larger the slope of the total energy $E_{\text{W}}(d)$, the more energy can be gained by relaxing the chain from a distance d to $\tilde{d}$. Therefore, large values of F_0 and small energy barriers ΔE_{lead} will favor chain elongation.

When the number of atoms in the chain N is very large, we can safely assume $\epsilon(d) - \epsilon(\tilde{d}) \approx \frac{\delta\epsilon(d)}{\delta d} \cdot \delta d = F(d) \cdot \delta d$, where $\delta d = d - \tilde{d} \approx \frac{L}{N^2}$, and the P-criterion reads

$$F(d) \geq \frac{\Delta E_{\text{lead}} + \epsilon(d)}{d} = f(d) \tag{4}$$

where $f(d)$ is the generalized string tension, or the work done in drawing the chain with interatomic distance d out of the lead per unit chain length. This equation provides the interval of distances in which the suspended chain can be producible. Analysis of the producibility of the long wires and chains in terms of the generalized string tension has been successfully performed in the past [1, 19, 32, 33]. It is easy to demonstrate that the lower and upper boundaries of the interval of distances where the chain is producible and equation (4) is satisfied correspond to the local minimum and maximum of $f(d)$, respectively.

5. Impurity-assisted chain formation in break junctions

In this section we address the question of the impact of light s and p impurities H, C, N, and O on the producibility of noble-metal chains in an MCBJ. A key towards understanding the impurity-assisted formation process is the additional degree of freedom of lateral relaxation in zigzag bonds, which can be incorporated into the criterion for producibility formulated in section 4.

Before analyzing the results of our extended model, it is important to discuss crucial energy scales determining the elongation process. While the extraction of atoms out of the leads can be modeled in line with previous studies [1, 19], we have to consider additionally the supplementing of the pure chain with the impurities. Here, we assume that the light impurities H, C, N, and O are present in the atmosphere and are not bound at the surface. This assumption is well justified considering that the concentration of such impurities is controlled by the partial pressure in experiments. Furthermore, *a priori*, the dissociation energy of impurity molecules potentially acts as an additional barrier in the energetic balance given by relation (1). Here we refer to the results by Bahn *et al* [12], who reported the chemisorption energy of Au chains to be of the order of -1.5 eV per O atom pair with respect to the energy of the free O_2 molecule.

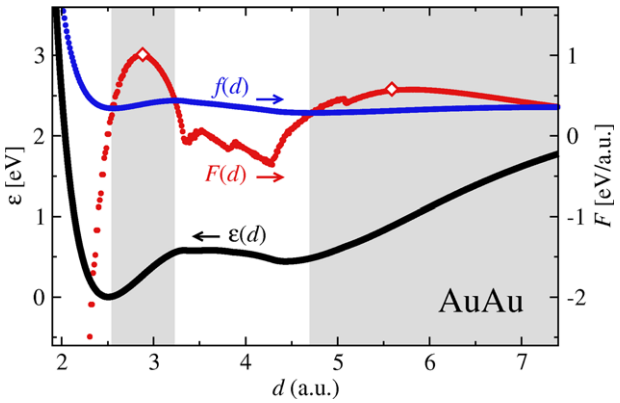

Figure 6. Binding energy $\varepsilon(d)$, force $F(d)$ and generalized string tension $f(d)$ for a pure zigzag Au chain. Both local maxima of $F(d)$ are marked with open diamonds and will be referred to as break forces F_0. The gray shaded areas represent regions where $f(d) > F(d)$ and the criterion for producibility is fulfilled.

This finding of highly preferential binding of impurity atoms to the chain allows for two important simplifications. Firstly, impurities have a strong tendency to cover all assisted bonds of the chain atoms. Hence, the resulting structure is well described by a chain of alternating Au and O atoms. Secondly, we assume that the dissociation of impurity molecules and absorption to the metal bonds happens instantaneously after an additional metal atom has joined the chain. Additionally, since the chemisorption energy of the molecules is negative, it effectively lowers the energy barrier for the lead atom to enter the chain. Since we do not include this effect into the energetics considerations, our conditions for chain elongation are thus more stringent, which makes the conclusions of our work more sound. The values for the energy barriers we use here (introduced as ΔE_{lead} in section 4) constitute 0.86 eV, 0.75 eV and 1.16 eV for Au, Ag and Cu, respectively.

Next, for a Au chain in the thermodynamic limit ($N \to \infty$) we introduce some important general concepts necessary for a detailed analysis of the results. As is apparent from figure 6 and equation (4), two distinct regions of producibility can arise: one in the domain of zigzag chains (angle $\alpha > 0$), and the second in the region of straight chains (angle $\alpha \approx 0$). Accordingly, in both regimes the maximal sustainable force F_0 is observed at two different values of the inflection point $\hat{d}$. Additionally, while both parameters undergo large changes depending on the system, F_0 and $\hat{d}$ of the straight chains have a clear physical meaning and can provide important understanding of the most general trends of the chain formation. Hence, if not specified explicitly, F_0 and $\hat{d}$ will refer to the straight chain domain from here on.

The most obvious influence of the considered impurities on the elongation process can be seen in the changes in the break force F_0 when compared to the case of the pure chains. From figure 7, in which the break force for each of the studied cases is given, we first of all observe that in pure noble-metal chains a stronger binding and correspondingly larger values of F_0 occur for Au and Cu, while Ag chains have the weakest binding. This is a direct consequence of the shallower energy profiles for Ag chains, discussed in section 3. The fact that

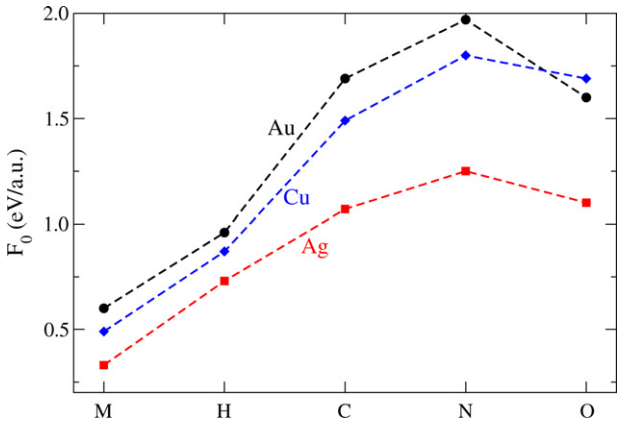

Figure 7. Break force F_0 for Au, Ag, and Cu pure and impurity-assisted chains. Along the *x*-axis 'M' labels the pure chain, while 'H', 'C', 'N', and 'O' label chains with corresponding impurities.

Au chains exhibit the largest value of F_0 among all NMs is in direct correspondence to experiments [2, 1]. When environmental impurities are added to the system, the bonds in all cases become stronger and the break forces larger owing to the pronounced covalent bonding in NM–X chains, as compared to the metallic binding in pure chains. Noticeably, among all impurities H atoms cause the smallest strengthening of the bonds, considering an absence of directionality of s orbitals, in contrast to the case of p impurities. On the other hand, adding p impurities to the NM chains leads to an approximately three-fold increase in the break force. Here, the most significant influence on F_0 can be seen for NM chains with nitrogen impurities, owing to the half-filled p shell of N atoms and the fact that the major contribution to the bonding in NM chains with p impurities comes from the interaction of the p electrons of the impurity with the half-filled s–d_{z^2} shell of the noble-metal chain.

Next, we perform a detailed analysis of the criterion of producibility for the NM and NM–X chains, as given by equation (2). In figure 8 we plot the energy, E^*, as a function of the interatomic distance in the chain, d, and the number of chain atoms, N, for both pure NM chains as well as NM chains with H, C, N and O impurities. The region of the (N, d) phase space where $E^* > 0$ provides the parameters of the chain configuration for which the elongation by one atom, or one NM–X pair of atoms, is possible. Additionally, the absolute value of the E^* energy gives an estimate of how probable or how improbable the event of elongation is. Correspondingly, in figure 8 the absolute value of E^* is given with appropriate color coding. The ability to estimate the E^* value is extremely useful, since in experiments the energy barrier for an atom to enter the chain can fluctuate, depending on the geometry of the contacts. Therefore, high positive values of E^* provide higher credibility to the occurrence of a single event of chain elongation at a particular point in the phase diagram for which the P-criterion is satisfied.

An important aspect of the chain creation process to consider is the stability of the suspended chains. The chain's stability in a break junction is a very complicated issue, since here the primary importance is due to the interplay of the local tip geometry, the phonon spectra of the finite chains, as well as the temperature and applied bias. Modeling of the chain's breaking process is therefore a highly non-trivial task, which is specific to each attempt at chain formation, and which cannot be undertaken in the present study. Here, we restrict ourselves to a simple but rather transparent way of quantifying the stability of the chains by referring to the value of their inflection point, $\hat{d}$, i.e. the interatomic distance at which the maximal force F_0 is sustained. The value of $\hat{d}$, which can be interpreted as the minimal interatomic distance at which the chain will be broken for a given N, is presented for each of the cases by a thick vertical line in the phase diagram of figure 8. As we can see for pure NM chains in figure 8, the position of the boundary of the P-region with respect to $\hat{d}$ is very similar for Cu, Ag and Au. On the other hand, for NM–X chains, the value of $\hat{d}$ varies in a comparatively narrow interval of distance between 7.9 and 8.9 bohr. This means that the properties of the considered chains with respect to their stability are comparatively constant. This observation is in accordance with a previous finding of [1] in which the stability of linear suspended 5d transition-metal chains was analyzed within a better approximation.

Let us first take a closer look at the phase diagrams for pure NM chains in figure 8. First we observe that all chains exhibit large areas of producibility, for both linear and zigzag geometries. This is a striking new finding, which implies that in the general case of even more complex geometries of suspended wires more than one structurally stable phase favoring chain elongation can co-exist. This suggests that in experiment the co-existence of such phases can be used to enhance the elongation properties of the chains by switching from one phase to another. For example, for considered chains, the switching from the linear region of producibility into the zigzag region of producibility can be achieved by pushing the electrodes towards each other, reducing thus the interatomic distance in the chain. On the other hand, the switching from the zigzag into the linear region of producibility can be achieved by pulling the electrodes apart quickly enough, such that the extraction of the atom from the lead into the chain and the corresponding reconstruction of the break junction does not occur. This technique can be particularly efficient, given that the stability of the phases and the respective elongation probabilities (proportional to E^*) can depend strongly on the details of the particular elongation attempt.

Secondly, we observe that chains consisting of more than 10 atoms can be described very well in the thermodynamic limit. Such a length scale is rarely reached in experiment [34], however, which underlines the importance of analyzing chain creation trends as a function of N. Here, the description of the chain formation process at its initiation with one to three atoms in the chain is clearly improved by extending the chain formation model [1] to zigzag geometries: the strict assumption of linear bonds leads to an additional cost in energy for relaxations below the equilibrium interatomic distance. In our extended model, the chains relax at such short interatomic distances into a zigzag geometry

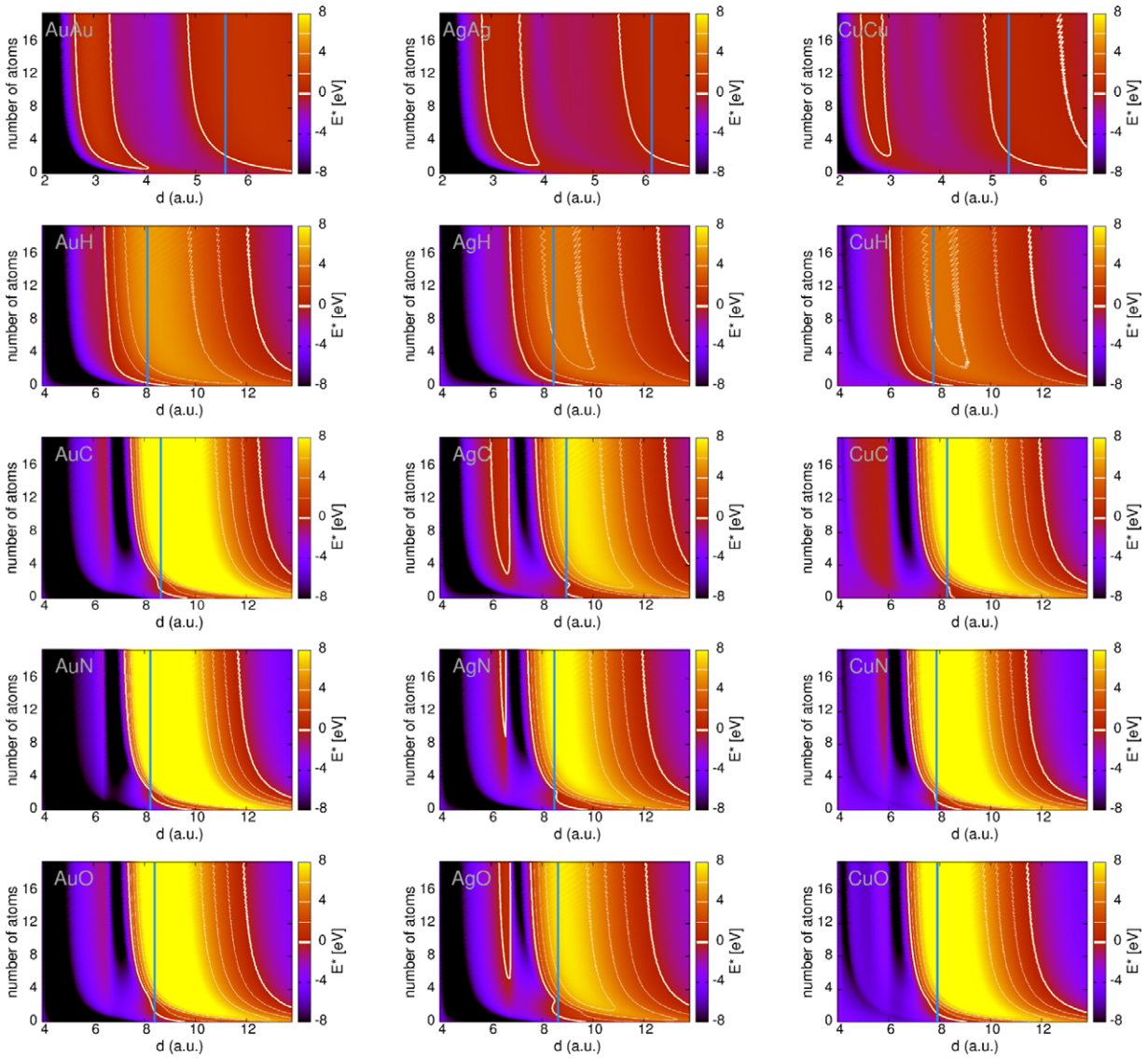

Figure 8. The energy landscape $E^*(d, N)$ as a function of the interatomic distance (d) and the number of atoms in the chain (N) describing the chain producibility for pure and impurity-assisted noble-metal chains, where E^* is defined by the criterion for producibility, equation (2). From left to right Au, Ag and Cu chains are displayed, from top to bottom, pure wires and H-, C-, N- and O-assisted chains. The thick white lines mark the $E^* = 0$ isolines indicating regions of producibility ($E^*(d, N) > 0$). Additional thin isolines are drawn at $E^*(d, N) = 2$, 4, 6, and 8 eV in each panel. Note that regions which are outside of the interval [−8 eV, 8 eV] are shown in the same color coding as the minimal and maximal values of this interval. To rate the stability of chains, for each panel the inflection point $\hat{d}$ in the linear regime of the binding energy potential is depicted by a thick blue vertical line.

with a comparable or even favorable energy contribution. Consequently, for Ag and Au the criterion for producibility can be fulfilled for smaller N. Generally speaking, this underlines the importance of structural versatility in a break junction experiment for chain elongation. Thirdly, both the linear and the zigzag phases of producibility have largest values of E^* energy for Au. The corresponding areas become less extended and exhibit somewhat smaller values of E^* when going from Ag to Cu. This trend can be directly related to the values of F_0 in figure 7 and their interplay with ΔE_{lead}.

Going now to NM chains with H impurities (second panel in figure 8), we observe wide regions of producibility only in the linear regime for all metals, in accordance with small ground state zigzag angles in this case. Also, while the width of the P-region is roughly the same for Cu, Ag and Au, the probability of chain elongation, characterized by the energy E^*, is noticeably larger for Au than for Ag and Cu. In any case, the E^* values, reaching as much as 5 eV for Au, are significantly larger than the corresponding values for pure chains. Additionally, for all N the area of producibility can be entered upon increasing the interatomic distance in the chain without exceeding the inflection point. Overall, this leads to the prediction of a strongly enhanced tendency towards chain formation and elongation in NM break junctions with H in the atmosphere.

Finally, we turn to the case of NM chains with p impurities C, N and O (the three lower panels of figure 8). As we have analyzed previously, adding p impurities to the

NM chains results in a three-fold increase in the values of the break force (figure 7). This results in very wide regions of producibility for all chains with very high values of E^* reaching over a threshold of 8 eV. These values are significantly larger than those for pure chains and even for chains with H adatoms. While the width of the P-region in the linear regime is similar for all NMs, the values of E^* are somewhat smaller for Ag than for Cu and Au, which can be attributed to the different break forces for these elements, see figure 7. Characteristically, for all cases the part of the P-region in the linear regime for which the interatomic distance lies below the inflection point is significant, thus ensuring structurally stable elongation.

As is apparent from figure 3, in contrast to the case of Cu and Au, Ag chains with C, N and O impurities exhibit two pronounced energy minima for the zigzag and linear regimes, separated by a local energy maximum. In terms of the P-criterion this results in finite zigzag producibility regions for Ag, in addition to the P-region in the linear regime. Additionally, although the values of E^* are modest for zigzag chains, the area in the phase space where the zigzag chains can be elongated is clearly visible, especially for C- and O-assisted Ag chains. As discussed previously for pure chains, the second region of producibility can open the way to more efficient elongation. Despite the fact that shorter Ag chains can be grown in the linear regime only, for larger N rapid pushing of the tips towards each other might lead to a jump from the linear into the zigzag mode with further chain growth in the latter regime of higher stability. A clear indication of the zigzag-like areas can be also seen for smaller d in AuC, AuO, CuN, and in particular CuC cases, although the energy E^* is negative and reaches as much as -1 eV in these regions. Nevertheless, depending on the details of the chain growth and geometry of the tips, we believe that such regions can acquire positive energy E^* and lead to longer chains in analogy to break junctions of Ag. Overall, we conclude that the tendency to elongation of NM chains with p impurities is enhanced when compared to pure NM chains and NM chains with hydrogen.

6. Conclusions

We have presented a generalization of the model for the formation of zigzag and impurity-assisted chains in break junction experiments. On the basis of the extended model we investigated the growth of noble-metal wires with H, C, N and O impurities, taking the input from first-principles calculations. Our most important observation is that impurity-assisted chain growth leads to a strongly enhanced tendency towards chain elongation, when compared to pure noble-metal chains. Moreover, we reveal a distinct difference between the influences of s and p type impurities on chain creation, finding that p impurities lead to a higher chain elongation probability owing to a strong directional bonding. Importantly, we predict that the existence of more than one stable phase favoring chain elongation can occur in some cases, and suggest that this phenomenon can be employed for the production of longer chains in experiments. By utilizing one of the most important advantages of our model we are able to translate our findings into phase diagrams for successful chain creation, explicitly providing the values for the interatomic distances and the lengths of the chains for which elongation can be achieved.

Acknowledgments

The authors kindly thank Professors J M van Ruitenbek and E Scheer for inspiring and fruitful discussions. YM gratefully acknowledges funding under the HGF-YIG Programme VH-NG-513 and SDN acknowledges funding from Conicet, PIP00258.

References

[1] Thiess A, Mokrousov Y, Blügel S and Heinze S 2008 *Nano Lett.* **8** 2144
[2] Smit R H M, Untiedt C, Yanson A I and van Ruitenbeek J M 2001 *Phys. Rev. Lett.* **87** 266102
[3] Ryu M and Kizuka T 2006 *Japan. J. Appl. Phys.* **45** 8952
[4] Ohnishi H, Kondo Y and Takayanagi K 1998 *Nature* **395** 780
[5] Yanson A I, Rubio-Bollinger G, van den Brom H E, Agraït N and van Ruitenbeek J M 1998 *Nature* **395** 783
[6] Rubio-Bollinger G, Bahn S R, Agraït N, Jacobsen K W and Vieira S 2001 *Phys. Rev. Lett.* **87** 026101
[7] Thijssen W H A, Marjenburgh D, Bremmer R H and van Ruitenbeek J M 2006 *Phys. Rev. Lett.* **96** 026806
[8] Novaes F D, da Silva A J R, da Silva E Z and Fazzio A 2003 *Phys. Rev. Lett.* **90** 036101
[9] Barnett F D, Haekkinen H, Scherbakov A G and Landman U 2004 *Nano Lett.* **4** 1845
[10] Rodrigues V, Bettini J, Rocha A R, Rego L G C and Ugarte D 2002 *Phys. Rev.* B **65** 153402
[11] Novaes F D, da Silva A J R, da Silva E Z and Fazzio A 2006 *Phys. Rev. Lett.* **96** 016104
[12] Bahn S R, Lopez N, Norskov J K and Jacobsen K W 2002 *Phys. Rev.* B **66** 081405
[13] Legoas S B, Rodrigues V, Ugarte D and Galvão D S 2004 Contaminants in suspended gold chains: an *ab initio* molecular dynamics study *Phys. Rev. Lett.* **93** 216103
[14] Sánchez-Portal D, Artacho E, Junquera J, Ordejón P, García A and Soler J M 1999 Stiff monatomic gold wires with a spinning zigzag geometry *Phys. Rev. Lett.* **83** 3884–7
[15] Ayuela A, Puska M J, Nieminen R M and Alonso J A 2005 Charging mechanism for the bond elongation observed in suspended chains of gold atoms *Phys. Rev.* B **72** 161403
[16] Calzolari A, Cavazzoni C and Nardelli M B 2004 Electronic and transport properties of artificial gold chains *Phys. Rev. Lett.* **93** 096404
[17] Mokrousov Y, Bihlmayer G and Blügel S 2005 *Phys. Rev.* B **72** 045402
[18] www.flapw.de
[19] Thiess A, Mokrousov Y, Heinze S and Blügel S 2009 *Phys. Rev. Lett.* **103** 217201
[20] Thiess A, Mokrousov Y and Heinze S 2010 *Phys. Rev.* B **81** 054433
[21] Fernández-Seivane L, García-Suárez V M and Ferrer J 2007 *Phys. Rev.* B **75** 075415
[22] Sánchez-Portal D, Artacho E, Junquera J, García A and Soler J M 2001 *Surf. Sci.* **482–485** 1261
[23] Çakır D and Gülseren O 2011 Effect of impurities on the mechanical and electronic properties of Au, Ag, and Cu monatomic chain nanowires *Phys. Rev.* B **84** 085450

[24] Zarechnaya E Yu, Skorodumova N V, Simak S I, Johansson B and Isaev E I 2008 *Comput. Mater. Sci.* **43** 522
[25] Hobi E, Fazzio A and da Silva A J R 2008 Temperature and quantum effects in the stability of pure and doped gold nanowires *Phys. Rev. Lett.* **100** 056104
[26] Hasmy A, Rincón L, Hernández R, Mujica V, Márquez M and González C 2008 On the formation of suspended noble-metal monatomic chains *Phys. Rev.* B **78** 115409
[27] Amorim E P M, da Silva A J R, Fazzio A and da Silva E Z 2007 *Nanotechnology* **18** 145701
[28] Anglada E, Torres J A, Yndurain F and Soler J M 2007 *Phys. Rev. Lett.* **98** 096102
[29] Bahn S R and Jacobsen K W 2001 *Phys. Rev. Lett.* **87** 266101
[30] da Silva E Z, da Silva A J R and Fazzio A 2001 *Phys. Rev. Lett.* **87** 256102
[31] Skriver H L and Rosengaard N M 1992 *Phys. Rev.* B **46** 7157
[32] Kondo Y and Takayanagi K 2000 *Science* **289** 606
[33] Tosatti E, Prestipino S, Kostlmeier S, Dal Corso A and Di Tolla F D 2001 *Science* **291** 288
[34] Kizuka T 2008 *Phys. Rev.* B **77** 155401